RSC Advances

PAPER

View Article Online
View Journal | View Issue

Check for updates

Cite this: *RSC Adv.*, 2021, **11**, 7331

Ultralight hybrid silica aerogels derived from supramolecular hydrogels self-assembled from insoluble nano building blocks†

Zongjian Liu,[a] Ling Liu,[b] Zhenggen Zhong,[b] Yuanyuan Ran,[a] Jianing Xi*[a] and Jin Wang *[b]

Received 18th January 2021
Accepted 6th February 2021

DOI: 10.1039/d1ra00418b

rsc.li/rsc-advances

Supramolecular hydrogels are a type of hydrogel cross-linked by non-chemical bonds and they have been widely applied in the field of smart systems, sensors, tissue engineering, and controlled drug delivery. Most supramolecular hydrogels are formed by soluble molecules, polymers, and metal ions. In this work, supramolecular hydrogels self-assembled between two insoluble nano building blocks (ISNBBs), graphene oxide (GO) and amino-functionalized silica nanoparticles (SiO_2–NH_2), have been discovered and synthesized. The gelation conditions of the two ISNBBs have been investigated. A step further, ultralight hybrid silica aerogels are obtained by supercritical drying of the physical hydrogels. No visible volume shrinkage is observed, due to the fact that the hydrogel networks are formed by rigid ISNBBs. Thus the hybrid aerogels possess ultralow density (down to 7.5 mg cm^{-3}), high specific surface areas (178.6 m^2 g^{-1}), and extremely high porosity (99.6%). The present work shows an alternative strategy to design and synthesize supramolecular hydrogels and aerogels using predetermined building blocks, together with designable morphology and physical properties for the target aerogels.

Open Access Article. Published on 12 February 2021. Downloaded on 1/22/2026 10:07:03 PM.
This article is licensed under a Creative Commons Attribution-NonCommercial 3.0 Unported Licence.

Introduction

Supramolecular hydrogels (or physical hydrogels) are a type of network cross-linked by non-covalent interactions such as hydrogen bonding,[1] hydrophobic interactions,[2] van der Waals interactions,[3] electrostatic interactions,[4] and π–π interactions.[5] Due to their non-covalent nature, the supramolecular hydrogels are normally reversible soft materials and are considered to be potential materials to construct smart systems, such as stimuli-responsiveness triggered by pH, temperature, electronic field, magnetic field, and light. Thus, they have been widely investigated as biomaterials for use in tissue engineering, controlled drug delivery, and tissue repairs.[6–12]

Aerogels are highly porous materials that are generally synthesized by a two-step process, sol–gel transition (to obtain a porous network) and specific dying process (*e.g.* supercritical liquid drying, to remove liquid in gels while keep the volume and microstructure unchanged or with limited changes).[13–25] Aerogels exhibit various attractive properties such as extremely low density, low thermal conductivity, high specific surface areas, high porosity, and high pore volume. Thus, they have found potential applications in the fields of aerospace, catalysis, filtration, thermal insulation, electronics, sensors, water purification, tissue engineering, and drug delivery. Recently, significant progress in aerogels have been achieved. For example, eco-friendly cellulose aerogels that were capable for oil absorption and oil/water separation,[26–28] anisotropic cellulose nanofibril composite sponges that were able to be used as senor and electromagnetic interference shielding,[29] fibrous polyimide sponges and aerogels with superior mechanical and thermal properties,[30,31] anisotropic nanocellulose aerogels that were suitable for fast liquid transportation,[32] ultrablack aerogels for solar steam generation,[33,34] *etc.* have been prepared. Reviews on the comprehensive developments and applications of aerogels are also available.[13,14,35–37] Aerogels and hydrogels could be considered as the same porous network in different stages, that hydrogels are filled with water in their pores while aerogels are filled with air in their pores. Therefore, there are plenty of similarities between hydrogels and aerogels, such as the same porous structure, and the same potential applications as catalyst support, water purification absorbent, and drug delivery system. Nevertheless, differences can be observed between these two materials. For instance, hydrogels are reversible and stimuli-responsive, but the stimuli-responsiveness in aerogels are rare because the movements of molecules are restricted in the solid state.[10,11]

On the other hand, supramolecular hydrogels are normally formed by soluble precursors,[38–41] which are soluble in the

[a]*Department of Rehabilitation, Beijing Rehabilitation Hospital, Capital Medical University, Beijing 100144, P. R. China. E-mail: xijn999@ccmu.edu.cn*

[b]*Key Laboratory of Multifunctional Nanomaterials and Smart Systems, Suzhou Institute of Nano-Tech and Nano-Bionics, Chinese Academy of Sciences, Suzhou 215123, P. R. China. E-mail: jwang2014@sinano.ac.cn*

† Electronic supplementary information (ESI) available: SEM image of GO, photo image of supramolecular hydrogels, *etc.* See DOI: 10.1039/d1ra00418b

© 2021 The Author(s). Published by the Royal Society of Chemistry

Open Access Article. Published on 12 February 2021. Downloaded on 1/22/2026 10:07:03 PM.
This article is licensed under a Creative Commons Attribution-NonCommercial 3.0 Unported Licence.

molecular level when they form the hydrogel networks. Due to the weak connection of supramolecular hydrogels, their corresponding aerogels cannot be obtained because there are no preformed network to support their volumes and structures. Recently graphene oxide (GO) has been recognized as an attractive two dimensional building blocks for supramolecular hydrogels, which are insoluble dispersed nano plates and various GO-based supramolecular hydrogels have been prepared by different secondary interactions including hydrogen bonding, π–π stacking, electrostatic interaction, and coordination.[42–45] Cross-linkers been used to prepare GO based supramolecular hydrogels including poly(vinyl alcohol) (PVA), poly(ethylene oxide) (PEO), hydroxypropylcellulose (HPC), poly(vinyl pyrrolidone) (PVP), polyethylenimine (PEI), cetyltrimethyl ammonium bromide (CTAB), tetramethylammonium chloride (TMAC), and melamine. The cross-linkers are all soluble components so that they can efficiently form non-covalent interactions with GOs. Moreover, GOs can be self-assembled between themselves *via* π–π stacking through reduction, and their corresponding hydrogels can be successfully transferred to GO aerogels, which showed potential applications in energy storage and water purification.[46–49] Hybrid GO based hydrogels and aerogels incorporated with other insoluble nano building blocks (ISNBBs), such as MoS_2, carbon nanotubes (CNTs), and boron nitride (BN),[50–54] have been synthesized and they showed improved performances. Nevertheless, these ISNBBs did not act as cross-linkers for the GO to form supramolecular hydrogels, they acted as fillers that were embed in the GO matrix.

In this work, amino group ($-NH_2$) functionalized silica nanoparticles (SiO_2–NH_2) are synthesized and found to form hybrid supramolecular hydrogels with GO. The SiO_2–NH_2 nanoparticles played as cross-linkers and hydrogen bonds were formed between SiO_2–NH_2 and GO as illustrated in Fig. 1. Hybrid supramolecular hydrogels can be formed in a wide range of concentration. The supramolecular hydrogels were formed solely by ISNBBs, which formed interconnected network throughout the hydrogels. Herein, the gelation behaviour, parameter, and the corresponding hybrid aerogels will the systematically investigated.

Experimental

Materials

Graphite powder was purchased from Qingdao Tianheda Graphite Co., Ltd, Qingdao, China (purity 99.8%). 3-Aminopropyltriethoxysilane (APTES) (AR, purity 99%) and tetraethoxysilane (TEOS) (GR, purity 98%) were purchased from Aladdin Industrial Corporation, Shanghai, China. GO were prepared according to literatures by a modified Hummers method[42,55,56] and GO aqueous solution were diluted to various concentrations. Other reagents are of analytical purity and used as received.

Synthesis of SiO_2–NH_2 nanoparticles

SiO_2–NH_2 nanoparticles were synthesized through a revised Stöber method[57,58] as follows: to a mixture of 125 ml distilled water and 100 μl ammonium hydroxide, 10 ml TEOS was added under stilling for 2 h. Then, 1.5 ml APTES was added. SiO_2–NH_2 nanoparticles were formed as white precipitate and dried in vacuum. SiO_2–OH nanoparticles were synthesized *via* a Stöber method without the addition of APTES for comparison.

Synthesis of GO–SiO_2 supramolecular hydrogels and aerogels

GO–SiO_2 supramolecular hydrogels were synthesized by mixing GO aqueous solution and SiO_2–NH_2 nanoparticle aqueous

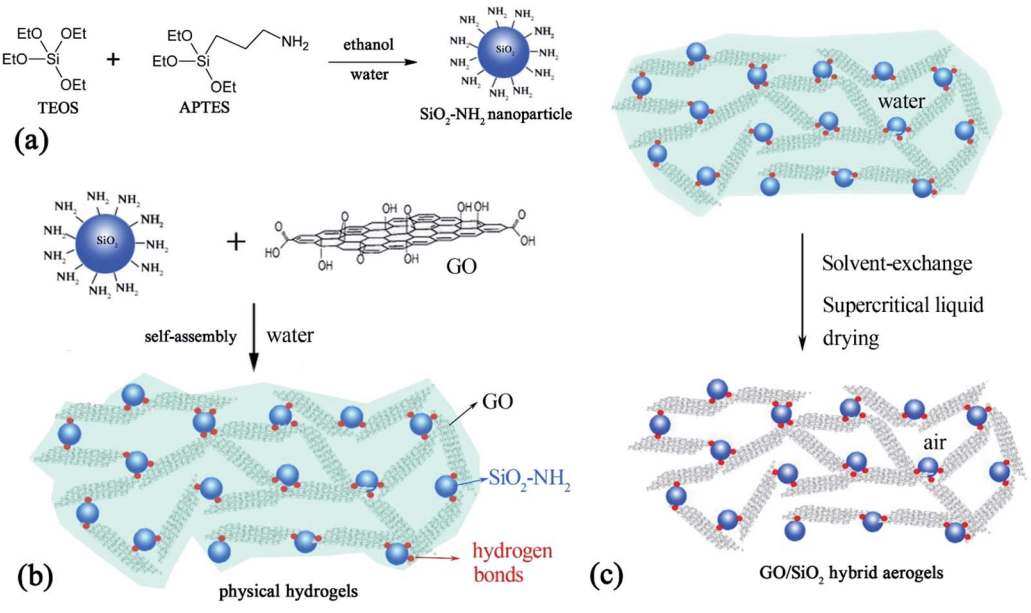

Fig. 1 (a) Schematic description of the synthesis of SiO_2–NH_2; (b) GO–SiO_2–NH_2 hybrid supramolecular hydrogels; and (c) the corresponding GO–SiO_2–NH_2 hybrid aerogels.

© 2021 The Author(s). Published by the Royal Society of Chemistry

Open Access Article. Published on 12 February 2021. Downloaded on 1/22/2026 10:07:03 PM.
This article is licensed under a Creative Commons Attribution-NonCommercial 3.0 Unported Licence.

solution, take the GO5–$SiO_2$15 for example: 1 ml fleshly prepared SiO_2–NH_2 aqueous solution (15 mg ml^{-1}) was mixed with 1 ml GO aqueous solution (5 mg ml^{-1}) and stirred for 5 min. Supramolecular hydrogels were formed in 2 h. The supramolecular hydrogels were named as GO*m*–SiO_2*n*, where *m* and *n* indicate the concentration of GO and SiO_2 nanoparticles, respectively. The supramolecular hydrogels were converted to aerogels by solvent-exchange with ethanol and supercritical CO_2 drying.

Characterization

Fourier transform infrared (FT-IR) spectra are recorded on a Nicolet iN10 spectrometer (Thermo Scientific, USA) in the reflection mode. The morphologies are observed on a field-emission scanning electron microscopy (FESEM, Quanta 400 FEG, USA), the samples are coated with Au nanoparticles at a current of 20 mA for 2 min in advance. TEM measurement was carried out on a Tecnai G2 F20 S-TWIN instrument. N_2 adsorption–desorption isotherms are performed on Micromeritics (ASAP 2020, USA). The specific surface area of the samples are determined by the Brunauer–Emmett–Teller (BET) method based on the amount of N_2 adsorbed at pressures $0.05 < P/P_0 < 0.3$. The pore volumes are measured at the point $P/P_0 = 0.99$. The pore size distribution and the average pore diameters are analyzed by the Barrett–Joyner–Halenda (BJH) method. Densities of the aerogels are calculated by weighting the samples and measuring the volumes.

Results and discussion

GO based hydrogels have attractive increasing interests and various cross-linkers can be used. Nevertheless, challenges remain for the self-assembly of GO with ISNBBs, while network formed by IsNBBs (such as metal nano spheres) show great potential for functional materials.[59] On the other hand, SiO_2 nanoparticles have found wide applications in catalyst, energy, environment, and biomedicine.[60–63] Since there are plenty of –OH groups on the surfaces of SiO_2 nanoparticles prepared by Stöber method, it could be interesting to see if GO and SiO_2 nanoparticles could be self-assembled into hydrogels, as it was happened between GO and PVA. However, hydrogels could not be formed between GO and SiO_2 nanoparticles. Interestingly, we found that –NH_2 functionalized SiO_2 nanoparticles could self-assembly with GO and form supramolecular hydrogels.

The synthetic approach of SiO_2–NH_2 nanoparticles is illustrated in Fig. 1a, which is a revised Stöber method that a diluted NH_3H_2O aqueous solution is used, then TEOS is added under stirring and there are no observable changes. After the addition of APTES, white precipitates were formed. APTES acted as both co-monomers to functionalize the silica nanoparticles with –NH_2 groups and as basic catalyst to promote the hydrolysis and condensation of TEOS.[64,65] As depicted in Fig. 1b, supramolecular hydrogels were formed after mixed GO and SiO_2–NH_2 nanoparticles aqueous solution. The only differences of the silica nanoparticles were the replacement of –OH with –NH_2, which may form stronger hydrogen bonds between GO and result in the formation of supramolecular hydrogels. After solvent-exchange with ethanol, hybrid aerogels (Fig. 1c) were synthesized by supercritical CO_2 drying.

Fig. 2 shows the morphology and the N_2 absorption–desorption isotherm of the SiO_2–NH_2 nanoparticles. As can be seen from the SEM image, SiO_2–NH_2 nanoparticles were spherical particles with diameters lower than 50 nm. The TEM image of the SiO_2–NH_2 nanoparticles shown in Fig. S1, ESI† further indicated that the diameter of them ranged from 20–40 nm. The specific surfaces area (SSA) of the SiO_2–NH_2 nanoparticles was determined to be 163 m^2 g^{-1}. The small size and large SSA value of the SiO_2–NH_2 nanoparticles may facilitate the formation of supramolecular hydrogels with GO, which significantly increased the contact areas between the two ISNBBs.

The gelation behaviour between GO and SiO_2–NH_2 nanoparticles are systematically investigated, and the results are presented in Fig. 3. GO were synthesized according to our previous work by a modified Hummers method,[55,56] the size of graphite powder was 30–40 μm. The SEM image of the GO is shown in Fig. S2, ESI.† They were diluted into difference concentrations as shown in Fig. 3. It can be seen that supramolecular hydrogels can be formed with a wide range of GO concentration from 2 mg ml^{-1} to 10 mg ml^{-1}, while the

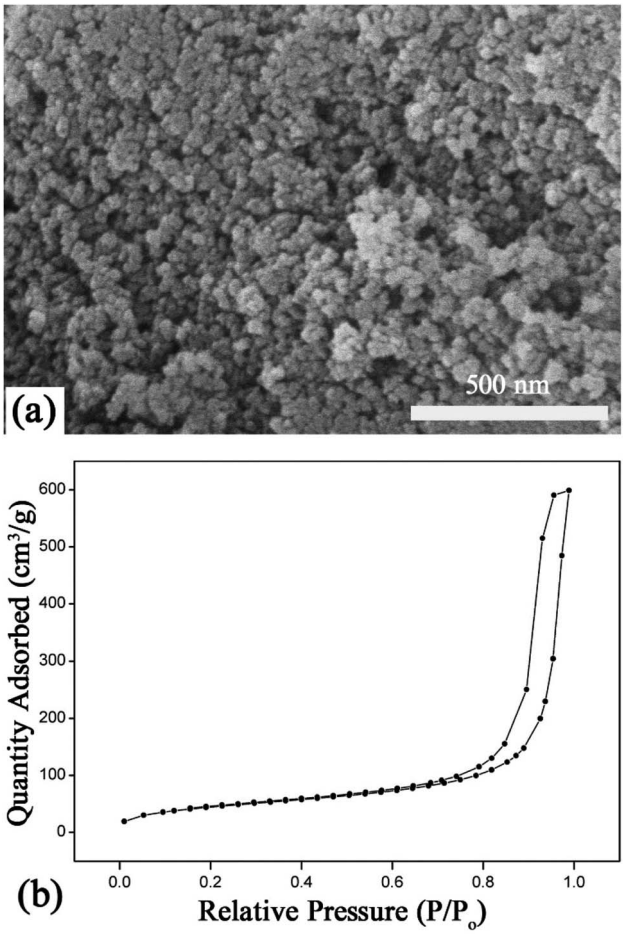

Fig. 2 (a) SEM image of SiO_2–NH_2 nanoparticles; (b) nitrogen absorption–desorption isotherm of the SiO_2–NH_2 nanoparticles.

Open Access Article. Published on 12 February 2021. Downloaded on 1/22/2026 10:07:03 PM.
This article is licensed under a Creative Commons Attribution-NonCommercial 3.0 Unported Licence.

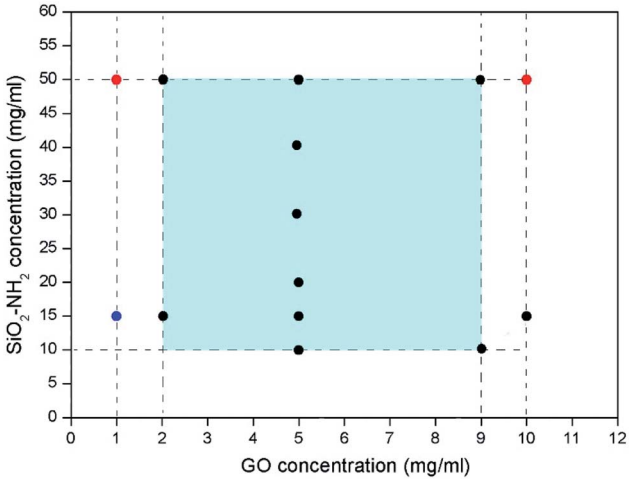

Fig. 3 Gelation conditions for the SiO_2–GO hybrid supramolecular hydrogels: black solid circle (●) indicated that supramolecular hydrogels were formed; red solid circle (●) indicated that hydrogel cannot be formed; blue circle (●) indicated that precipitates were formed; the light blue region suggest that supramolecular hydrogel may be formed.

concentration of SiO_2–NH_2 nanoparticles ranged from 10 mg ml^{-1} to 50 mg ml^{-1} (see Fig. S3, ESI† for the photo images of the hydrogels). When the concentration of the IsNBBs were located in the light blue region, supramolecular hydrogels would possibly be formed. It should be pointed out that when the concentration of SiO_2–NH_2 nanoparticles reached to 50 mg ml^{-1}, supramolecular hydrogels did not formed when the concentration of GO was 10 mg ml^{-1}. The dispersion of GO and SiO_2–NH_2 nanoparticles was difficult to homogenously mixed. When the concentration of GO was down to 1 mg ml^{-1}, hydrogels could also not be formed, instead precipitates were obtained when the concentration of SiO_2–NH_2 nanoparticles was 15 mg ml^{-1}. The results indicated that diluted GO dispersion (*e.g.* 1 mg ml^{-1}) cannot form continuous network throughout the mixture solution. Nevertheless, GO can still interconnected with SiO_2–NH_2 nanoparticles to form precipitates.

Since the supramolecular hydrogels were formed solely by ISNBBs, there must be phase separated network that could persist its porous structure to obtain the corresponding aerogels. Therefore, the supramolecular hydrogels were dried by supercritical CO_2, and GO–SiO_2 hybrid aerogels were successfully obtained (Fig. S4, ESI†). The density of the aerogels was down to 7.5 mg ml^{-1} for the GO5–$SiO_2$10 aerogels, which was equal to the theoretical density. Considering the negligible volume shrinkage of the aerogels, it could be concluded that there were no loss of GO and SiO_2–NH_2 nanoparticles during the solvent-exchange and supercritical liquid drying process. The nearly 100% yield, which is a superior aspect for aerogel prepared by ISNBBs. In contrast, GO aerogels that were cross-linked by π–π stacking *via* reduction of GO,[55,56] or cross-linked by soluble polymers such as PVA, PEO, and PVP,[46–49] were remarkably shrunk during both the solvent-exchange and drying processes.

According to the equation:[11]

$$\text{Porosity} = 1 - \rho_b/\rho_s$$

Where ρ_b is the bulk density of the aerogel, and ρ_s is the density of the skeleton of the aerogel. The porosity of the hybrid aerogels was calculated to be 99.6%.

The FTIR spectra of GO, SiO_2–NH_2 nanoparticles, and the hybrid aerogels are presented in Fig. 4. Peaks located at 2982 cm^{-1} could be clearly observed for the SiO_2–NH_2 nanoparticles, which can be ascribed to the C–H vibration from APTES groups. The broad and strong peak located at 3100–3400 cm^{-1} suggested the presence of –NH_2. The vibration peaks of Si–O–Si and Si–C can be observed at 1100 and 840 cm^{-1}, respectively. The vibration peaks of C=O stretching vibration in GO of the aerogel located at 1644 cm^{-1} (black arrow) showed a shift from 1720 cm^{-1} (red arrow), which indicated the formation of hydrogen bonds between GO and the SiO_2–NH_2 nanoparticles that resulted in the formation of supramolecular hydrogels.[66] In addition, the supramolecular hydrogel could be transferred into sol when temperature elevated up to 90 °C (Fig. S5a, ESI†), possibly due to the broken of hydrogen bonds between GO and SiO_2–NH_2. Besides, SiO_2–OH nanoparticles without –NH_2 groups were synthesized, and they could not form hydrogels with SiO_2–NH_2 (Fig. S5b, EIS†) and GO (Fig. S5c†). Those results indicated that the hydrogen bonds in the supramolecular hydrogels may be formed between –NH_2 (in SiO_2–NH_2) and –COOH groups (in GO).

The microstructure of the GO–SiO_2 hybrid aerogels is investigated by SEM. Fig. 5 shows the SEM image of GO5–$SiO_2$15 aerogels. Pore size up to 1 μm could be observed, and the pores were homogenously distributed. From the SEM image with larger magnification times, SiO_2–NH_2 nanoparticles can be clearly identified and were found to be dispersed on the GO sheets without remarkable aggregation.

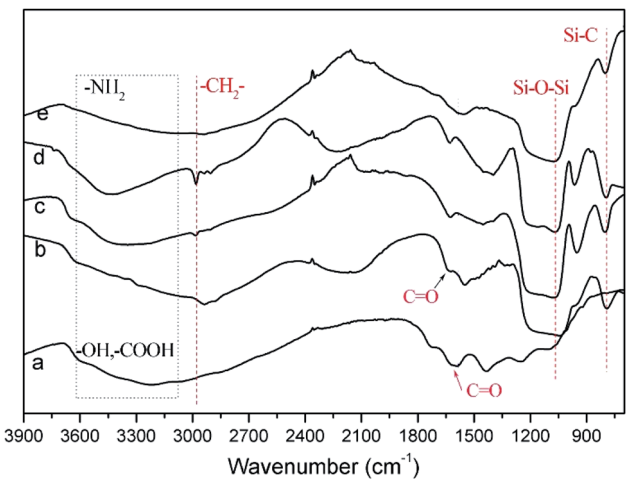

Fig. 4 FT-IR spectra of (a) GO; (b) GO5–$SiO_2$10 hybrid aerogels; (c) GO5–$SiO_2$15 hybrid aerogels; (d) GO5–$SiO_2$20 hybrid aerogels; (e) SiO_2–NH_2 nanoparticles.

© 2021 The Author(s). Published by the Royal Society of Chemistry

Open Access Article. Published on 12 February 2021. Downloaded on 1/22/2026 10:07:03 PM.
This article is licensed under a Creative Commons Attribution-NonCommercial 3.0 Unported Licence.

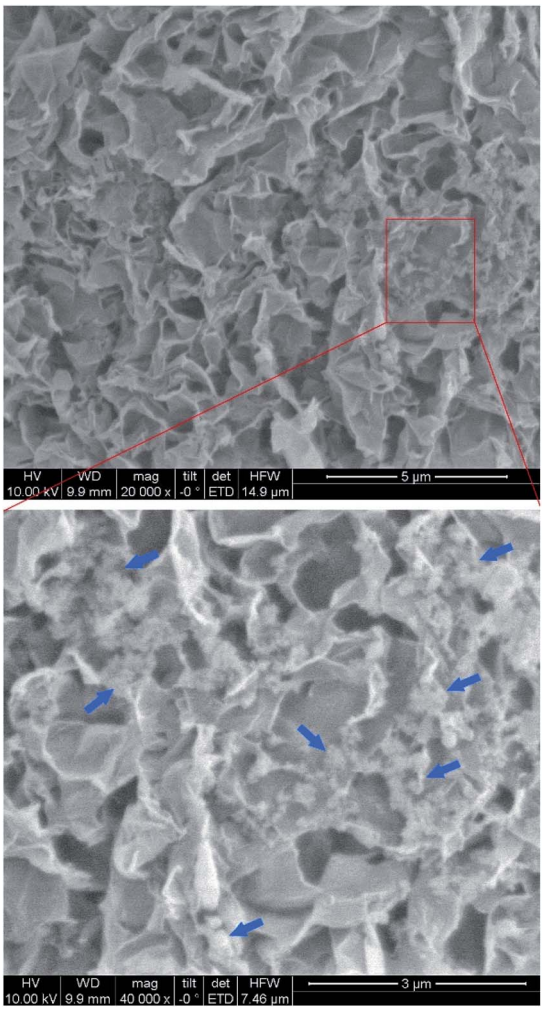

Fig. 5 SEM images of the GO5–$SiO_2$15 hybrid aerogels, blue arrows pointed to the SiO_2–NH_2 nanoparticles.

The results confirmed that GO were gelled cross-linked by SiO_2–NH_2 nanoparticles, as illustrated in Fig. 1b. Combine with the highly porous structure of the aerogel and hydrogels, the hybrid aerogels might be ideal candidate for tissue engineering and drug delivery matrix.

The N_2 adsorption–desorption isotherms and the pore size distribution curves of the hybrid aerogels are shown in Fig. 6. All the aerogels exhibited hysteresis loops, which were due to the typical features of mesoporous materials (type IV isotherms). The BET surface areas of the samples were 178, 120, 150 $m^2\ g^{-1}$ for the GO5–$SiO_2$10, GO5–$SiO_2$15, and GO5–$SiO_2$20 hybrid aerogels, respectively. All the aerogels possessed high pore volume ranged from 0.92 to 1.24 $cm^3\ g^{-1}$. Fig. 6b indicated that the aerogels also possessed mesopores, with average diameter of 43, 37, and 36 nm for GO5–$SiO_2$10, GO5–$SiO_2$15, and GO5–$SiO_2$20 hybrid aerogels, respectively. The SEM and BET results indicated that the hybrid aerogels possessed hierarchically pores ranged from tens of nanometers to several micrometers.

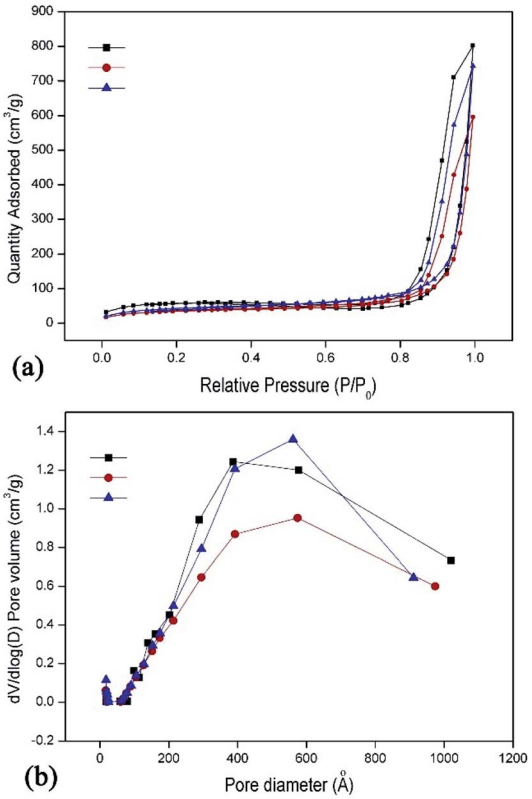

Fig. 6 (a) Nitrogen absorption–desorption isotherm of the hybrid aerogels; (b) pore distribution of the hybrid aerogels.

Conclusions

In conclusions, the gelation between GO and SiO_2–NH_2 nanoparticles, which are ISNBBs, have been observed. They can form supramolecular hydrogels in a wide range of concentration from 2 mg ml^{-1} to 10 mg ml^{-1} for GO and 10 mg ml^{-1} to 50 mg ml^{-1} for SiO_2–NH_2 nanoparticles. The framework of the supramolecular hydrogels were build up with GO and silica nanoparticles, where silica nanoparticles were dispersed on the GO nanosheet and acted as cross-linkers through the formation of hydrogen bonds between –NH_2 and –COOH groups in SiO_2–NH_2 and GO, respectively. Interestingly, the hybrid hydrogels could be successfully transferred into hybrid aerogels without observable volume shrinkage. The aerogels exhibited extremely low density of 7.5 mg ml^{-1}, large pore volume of 1.24 $cm^3\ g^{-1}$, high porosity of 99.6%, and high BET SSA ranged from 120–178 $m^2\ g^{-1}$. In addition, the aerogels possessed hierarchically porous structures from tens of nanometers to several micrometers, combined with the excellent biocompatibility of GO and SiO_2, the stimuli responsive behaviours, these supramolecular hydrogels and aerogels may find useful application in biomedicine, such as drug carriers and tissue engineering. The results also indicated that hydrogels and aerogels could be synthesised from ISNBBS with predetermined structure and properties.

© 2021 The Author(s). Published by the Royal Society of Chemistry

Open Access Article. Published on 12 February 2021. Downloaded on 1/22/2026 10:07:03 PM. This article is licensed under a Creative Commons Attribution-NonCommercial 3.0 Unported Licence.

Author contributions

Z. Liu and L. Liu completed the experiment and analyzed the data. Z. Zhong contributed to formal analysis. J. Wang designed and supervised the project. J. Xi supervised the project. Z. Liu wrote the original draft, and all the author reviewed and edited the manuscript.

Conflicts of interest

There are no conflicts to declare.

Acknowledgements

This work was financially supported by the National Natural Science Foundation of China (91963124, 51773225, 81671161).

Notes and references

1 Y. Zhao, Z. Li, Q. Li, L. Yang, H. Liu, R. Yan, L. Xiao, H. Liu, J. Wang, B. Yang and Q. Lin, *Macromol. Rapid Commun.*, 2020, **41**, 2000441.
2 H. Xiong, Y. Li, H. Ye, G. Huang, D. Zhou and Y. Huang, *J. Mater. Chem. B*, 2020, **8**, 10309–10313.
3 Y. Yan, A. Keizer, A. A. Martens, C. L. P. Oliveira, J. S. Pedersen, F. A. de Wolf, M. Drechsler, M. A. C. Stuart and N. A. M. Besseling, *Langmuir*, 2009, **25**, 12899–12908.
4 J. Li, Z. Su, X. Ma, H. Xu, Z. Shi, J. Yin and X. Jiang, *Mater. Chem. Front.*, 2017, **1**, 310–318.
5 S. K. Mandal, T. Kar and P. K. Das, *Chem.–Eur. J.*, 2013, **19**, 12486–12496.
6 A. Hoque, N. Sangaj and S. Varghese, *Macromol. Biosci.*, 2019, **19**, 1800259.
7 X. Dou, N. Mehwish, C. Zhao, J. Liu, C. Xing and C. Feng, *Acc. Chem. Res.*, 2020, **53**, 852–862.
8 L. Voorhaar and R. Hoogenboom, *Chem. Soc. Rev.*, 2016, **45**, 4013–4031.
9 A. Rey-Rico and M. Cucchiarini, *Polymers*, 2019, **11**, 514.
10 J. Wang, Q. Fang, L. Ye, A. Zhang and Z. G. Feng, *Soft Matter*, 2020, **16**, 5906–5909.
11 J. Wang and X. Zhang, *ACS Nano*, 2015, **11**, 11389–11397.
12 S. Qie, Y. Hao, Z. Liu, J. Wang and J. Xi, *Acta Chim. Sin.*, 2020, **78**, 232–244.
13 S. Jiang, S. Agarwal and A. Greiner, *Angew. Chem., Int. Ed.*, 2017, **56**, 15520–15538.
14 J. Wang and J. Wang, *Acta Chim. Sin.*, 2021, DOI: 10.6023/A20110531.
15 N. Hüsing and U. Schubert, *Angew. Chem., Int. Ed.*, 1998, **37**, 22–45.
16 R. Ciriminna, A. Fidalgo, V. Pandarus, F. Béland, L. M. Ilharco and M. Pagliaro, *Chem. Rev.*, 2013, **113**, 6592–6620.
17 M. Antonietti, N. Fechler and T. P. Fellinger, *Chem. Mater.*, 2014, **26**, 196–210.
18 A. C. Pierre and G. M. Pajonk, *Chem. Rev.*, 2002, **102**, 4243–4265.
19 J. P. Randall, M. A. B. Meador and S. C. Jana, *ACS Appl. Mater. Interfaces*, 2011, **3**, 613–626.
20 C. Ziegler, A. Wolf, W. Liu, A. K. Herrmann, N. Gaponik and A. Eychmüller, *Angew. Chem., Int. Ed.*, 2017, **56**, 13200–13221.
21 Z. Liu, Y. Ran, J. Xi and J. Wang, *Soft Matter*, 2020, **16**, 9160–9175.
22 J. Wang, X. Wang and X. Zhang, *J. Mater. Chem. A*, 2017, **5**, 4308–4313.
23 J. Wang, Y. Zhang and X. Zhang, *J. Mater. Chem. A*, 2016, **4**, 11408–11415.
24 J. Wang, R. Du and X. Zhang, *ACS Appl. Mater. Interfaces*, 2018, **10**, 1468–1473.
25 J. Wang, Y. Zhang, Y. Wei and X. Zhang, *Microporous Mesoporous Mater.*, 2015, **218**, 192–198.
26 Q. Shang, J. Chen, X. Yang, C. Liu, Y. Hu and Y. Zhou, *J. For. Eng.*, 2019, **4**, 105–111.
27 L. Zhou, H. Zhou, J. Li, S. Tan, P. Chen and Z. Xu, *J. For. Eng.*, 2019, **4**, 67–73.
28 Q. Shang, Y. Hu, C. Liu, X. Yang and Y. Zhou, *J. For. Eng.*, 2019, **4**, 86–92.
29 Y. Chen, L. Zhang, C. Mei, Y. Li, G. Duan, S. Agarwal, A. Greiner, C. Ma and S. Jiang, *ACS Appl. Mater. Interfaces*, 2020, **12**, 35513–35522.
30 S. Jiang, J. Y. Cheong, J. S. Nam, I. Kim, S. Agarwal and A. Greiner, *ACS Appl. Mater. Interfaces*, 2020, **12**, 19006–19014.
31 X. Li, J. Wang, Y. Zhao and X. Zhang, *ACS Appl. Mater. Interfaces*, 2018, **10**, 16901–16910.
32 Y. Chen, L. Zhou, L. Chen, G. Duan, C. Mei, C. Huang, J. Han and S. Jiang, *Cellulose*, 2019, **26**, 6653–6667.
33 H. Wang, A. Du, X. Ji, C. Zhang, B. Zhou, Z. Zhang and J. Shen, *ACS Appl. Mater. Interfaces*, 2019, **11**, 42057–42065.
34 M. Tan, J. Wang, W. Song, J. Fang and X. Zhang, *J. Mater. Chem. A*, 2019, **7**, 1244–1251.
35 A. Du, B. Zhou, Z. Zhang and J. Shen, *Materials*, 2013, **6**, 941–968.
36 L. Hu, R. He, H. Lei and D. Fang, *Int. J. Thermophys.*, 2019, **40**, 39.
37 A. Lamy-Mendes, R. F. Silva and L. Durães, *J. Mater. Chem. A*, 2018, **6**, 1340–1369.
38 X. Du, J. Zhou, J. Shi and B. Xu, *Chem. Rev.*, 2015, **115**, 13165–13307.
39 D. Xia, P. Wang, X. Ji, N. M. Khashab, J. L. Sessler and F. Huang, *Chem. Rev.*, 2020, **120**, 6070–6123.
40 G. Yu, K. Jie and F. Huang, *Chem. Rev.*, 2015, **115**, 7240–7303.
41 Q. Li, J. Wang, L. Ye, A. Zhang, X. Zhang and Z. G. Feng, *ChemNanoMat*, 2019, **5**, 838–846.
42 Z. Xu and C. Gao, *ACS Nano*, 2011, **5**, 2908–2915.
43 D. Chen, H. Feng and J. Li, *Chem. Rev.*, 2012, **112**, 6027–6053.
44 V. C. Tung, M. J. Allen, Y. Yang and R. B. Kaner, *Nat. Nanotechnol.*, 2009, **4**, 25–29.
45 H. Bai, C. Li, X. Wang and G. Shi, *J. Phys. Chem. C*, 2011, **115**, 5545–5551.
46 E. Greco, J. Shang, J. Zhu and T. Zhu, *ACS Omega*, 2019, **4**, 20948–20954.
47 L. A. Huang, Z. S. He, J. F. Guo, S. E. Pei, H. B. Shao and J. M. Wang, *ChemElectroChem*, 2019, **6**, 2698–2706.

© 2021 The Author(s). Published by the Royal Society of Chemistry

Open Access Article. Published on 12 February 2021. Downloaded on 1/22/2026 10:07:03 PM.
This article is licensed under a Creative Commons Attribution-NonCommercial 3.0 Unported Licence.

48 A. Plyushch, T. L. Zhai, H. S. Xia, C. Santillo, L. Verdolotti, M. Lavorgna and P. Kuzhir, *Materials*, 2019, **12**, 213.
49 W. K. Wang, Y. H. Wu, Z. W. Jiang, M. Z. Wang, Q. C. Wu, X. Zhou and X. W. Ge, *Chin. Chem. Lett.*, 2018, **29**, 931–934.
50 Y. Zhong, T. Shi, Y. Huang, S. Cheng, G. Liao and Z. Tang, *Nanoscale Res. Lett.*, 2019, **14**, 85.
51 F. Jiang, H. Liu, Y. Li, Y. Kuang, X. Xu, C. Chen, H. Huang, C. Jia, X. Zhao, E. Hotz, Y. Zhou, R. Yang, L. Cui and L. Hu, *ACS Appl. Mater. Interfaces*, 2018, **10**, 1104–1112.
52 B. Lee, S. Lee, M. Lee, D. H. Heong, Y. Baek, J. Yoon and Y. H. Kim, *Nanoscale*, 2015, **7**, 6782–6789.
53 M. Wang, T. Zhang, D. Mao, Y. Yao, X. Zeng, L. Ren, Q. Cai, S. Mateti, L. H. Li, X. Zeng, G. Du, R. Sun, Y. Chen, J. Xu and C.-P. Wong, *ACS Nano*, 2019, **13**, 7402–7409.
54 F. An, X. Li, P. Min, H. Li, Z. Dai and Z. Z. Yu, *Carbon*, 2018, **126**, 119–127.
55 G. Li, X. Zhang, J. Wang and J. Fang, *J. Mater. Chem. A*, 2016, **4**, 17042–17049.
56 R. Sun, G. Li, W. He, J. Wang, Q. Song and X. Zhang, *Adv. Mater. Interfaces*, 2016, **3**, 1600541.
57 W. Stöber and A. Fink, *J. Colloid Interface Sci.*, 1968, **26**, 62–69.
58 Y. Zhang, J. Wang and X. Zhang, *J. Colloid Interface Sci.*, 2018, **515**, 1–9.
59 Y. Zhang, J. Wang, Y. Wei and X. Zhang, *New J. Chem.*, 2017, **41**, 1953–1958.
60 T. Li, S. Shi, S. Goel, X. Shen, X. Xie, Z. Chen, H. Zhang, S. Li, X. Qin, H. Yang, C. Wu and Y. Liu, *Acta Biomater.*, 2019, **89**, 1–13.
61 S. Sivasankar and S. Chu, *Nano Lett.*, 2007, **7**, 3031–3034.
62 M. Xuan, Z. Wu, J. Shao, L. Dai, T. Si and Q. He, *J. Am. Chem. Soc.*, 2016, **138**, 6492–6497.
63 D. Tam, C. E. Ashley, M. Xue, E. C. Carnes, J. I. Zink and C. J. Brinker, *Acc. Chem. Res.*, 2013, **46**, 792–801.
64 Y. Wei, J. Wang, Y. Zhang, L. Wang and X. Zhang, *RSC Adv.*, 2015, **5**, 91407–91413.
65 J. Wang, Y. Wei, W. He and X. Zhang, *RSC Adv.*, 2014, **4**, 51146–51155.
66 D. C. Marcano, D. V. Kosynkin, J. M. Berlin, A. Sinitskii, Z. Sun, A. Slesarev, L. B. Alemany, W. Lu and J. M. Tour, *ACS Nano*, 2010, **4**, 4806–4814.

© 2021 The Author(s). Published by the Royal Society of Chemistry